

Post-Deposition Treatment of an Arylated-Carbazole Conjugated Polymer for Solar Cell Fabrication

Xiaofeng Liu, Wen Wen, and Guillermo C. Bazan*

Solution processable bulk heterojunction (BHJ) solar cells are emerging as potential low-cost alternatives for renewable energy generation.^[1–3] Considerable efforts have been taken in recent years to pursue higher power conversion efficiencies (PCEs) through the design of narrow bandgap donor-conjugated polymers^[4–6] and device optimization.^[7–9] Donor material development continues to dominate research, although efforts to find fullerene alternatives are notable.^[10–12] An important challenge is designing conjugated polymers with relatively deep highest occupied molecular orbital (HOMO) energy levels (to optimize the open circuit voltage, V_{oc})^[13–15] and appropriate absorption profiles (to maximize the short circuit current, J_{sc}).^[16–19] The 2,7-carbazole unit has proven as an excellent electron-rich fragment to design appropriate backbone structures.^[13,20–23] One of the most well studied such carbazole copolymer, namely PCDTBT, has gained particular attention recently.^[13,21] The initial PCE reached 3.6% in a typical BHJ device with V_{oc} of 0.88 V, and has been subsequently improved to 6% by device structure optimization.^[22]

Despite the advantages of the BHJ structure, the PCEs can be limited by undesirable morphology within the photoactive layer.^[24,25] Although thermal annealing, solvent vapour treatment and high boiling-point additives are useful processing options to tailor the organization of the BHJ blend,^[26–28] these methods need delicate control of the experimental variables. Another strategy to improve PCE has emerged by incorporating a conjugated polyelectrolyte interlayer. This study revealed that polar solvent, such as methanol, has an independent positive effect on the device performance.^[29] Polar solvents are also thought to modify the crystallinity within P3HT-containing BHJ solar cells.^[30,31]

In this contribution, we focus our attention on the effect of polar solvent on BHJ device performance. To carry out our studies, we focused on a new donor polymer, namely poly[N-9'-3,5-bis(octyloxy)phenyl]-2,7-carbazole-alt-5,5-(4',7'-dithienyl-5',6'-bis(octyloxy)-2',1',3'-benzothiadiazole)] (PCX3), which is

structurally related to PCDTBT, as shown in **Scheme 1A**. The deep HOMO level of the polymer leads to a high V_{oc} of 0.96 V and a PCE of up to 3.9% when blended with [6,6]-phenyl-C71-butyric acid methyl ester (PC₇₁BM). The PCE can be further improved to 5.1% by simple post solvent treatment.

The synthetic route to the arylated carbazole monomer **6** and PCX3 is outlined in **Scheme 1B**. Initially, 3,5-dimethoxy-1-iodobenzene (**1**) was coupled with 2,7-dibromocarbazole (**2**) in the presence of copper(I) iodide leading to arylated carbazole precursor **3** in good yield. Demethylation of the methoxy groups was achieved by treating **3** with BBr₃. Octyloxy side chains were subsequently introduced by reaction of 1-bromo-octane with dihydroxy carbazole **4** under mild conditions to yield octyloxy substituted carbazole **5**. It is noted that octyloxy side chain substituted donor and acceptor units were designed to balance solubility, intermolecular packing, weight percentage of conjugated backbone and a coplanar configuration. The carbazole monomer **6** was synthesized by double lithiation of octyloxy carbazole **5** with *n*-butyllithium, followed by quenching with 2-isopropoxy-4,4,5,5-tetramethyl-1,3,2-dioxaborolane. The acceptor fragment 4,7-bis(5-bromothiophen-2-yl)-2,1,3-benzothiadiazole (**7**) was obtained following a high yield procedure adapted from the literature.^[32] Finally, both monomers were co-polymerized via a Suzuki-Miyaura coupling manner. As described previously,^[21] end-capping reaction was carried out by using bromobenzene and phenylboronic acid to improve polymer stability.^[33] After a series of purification procedures,^[34] PCX3 was obtained in ~90% yield. Characterization by NMR spectroscopy is provided in the Supporting Information (Figure S1). As collected from chloroform fractions, PCX3 can easily form free-standing films (Figure S2), and was determined to have a number average molecular weight (M_n) of 65 KDa and a polydispersity index (PDI) of 2.5 by using high-temperature (150 °C) gel permeation chromatography in 1,2,4-trichlorobenzene (TCB) (Figure S3). PCX3 is soluble at room temperature in common organic solvents, such as chloroform, chlorobenzene (CB), orthodichlorobenzene (ODCB) and TCB.

The absorption spectrum of PCX3 in ODCB at room temperature, shown in **Figure 1a**, exhibits two absorption peaks centered at 392 nm and 530 nm, which upon heating at 100 °C blue-shift to 388 nm and 518 nm, respectively. A film from ODCB solution (1% w/w) shows broadened absorption bands at 400 nm and 556 nm. The film absorption onset of 650 nm corresponds to an optical bandgap of 1.91 eV, which is comparable to that of PCDTBT.^[13] Cyclic voltammetry (CV, **Figure S4**) shows that PCX3 exhibits reversible oxidation and reduction processes at 0.60 V and -1.65 V, respectively, relative to the ferrocene/ferrocenium couple. The HOMO (-5.40 eV) and lowest unoccupied molecular orbital (LUMO, -3.15 eV) energy levels can thus be calculated from these electrochemical values.

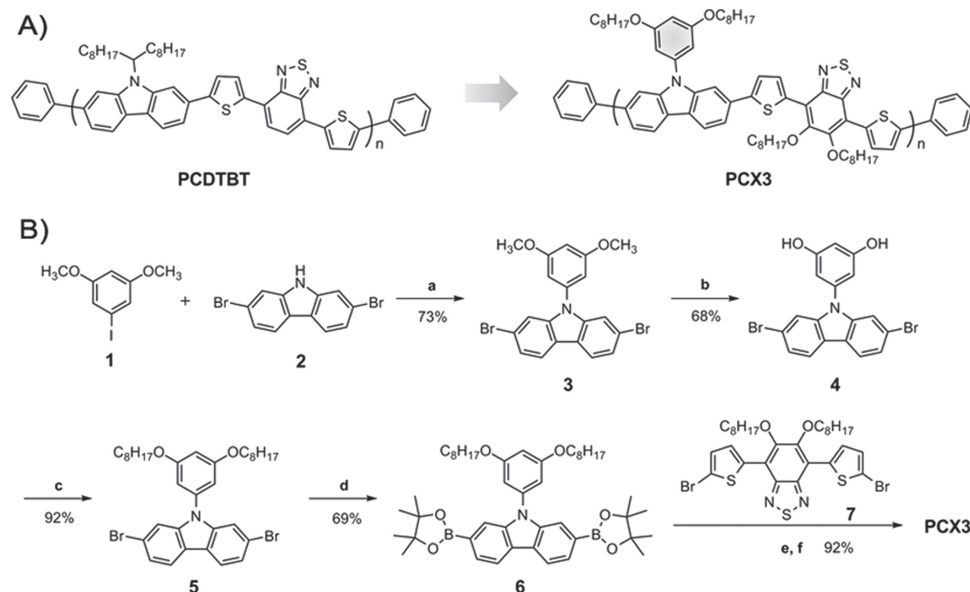
Dr. X. Liu,^[+] W. Wen,^[+] Prof. G. C. Bazan
Center for Polymers and Organic Solids
Department of Chemistry and Biochemistry
Department of Materials
University of California at Santa Barbara
Santa Barbara, California 93106, USA
E-mail: bazan@chem.ucsb.edu



W. Wen
State Key Laboratory of Electronic Thin Films and Integrated Devices
Department of Optoelectronic Information
University of Electronic Science and Technology of China (UESTC)
Chengdu 610054, P. R. China

[+] X.L. and W.W. contributed equally to this work.

DOI: 10.1002/adma.201201567



Scheme 1. (A) Chemical structures of PCDTBT and PCX3. (B) Synthetic route to carbazole monomer and PCX3. a) K_3PO_4 , CuI, (\pm)-trans-1,2-diaminocyclohexane, dioxane, 100 °C, overnight. b) BBr_3 , CH_2Cl_2 , -20 °C to r.t., 48 h. c) 1-Bromooctane, K_2CO_3 , DMF, 80 °C, 5 h. d) *n*-BuLi, THF, -78 °C, then 2-isopropoxy-4,4,5,5-tetramethyl-1,3,2-dioxaborolane, r.t., overnight. e) $Pd_2(dba)_3$, $P(o-tol)_3$, Et_4NOH (20% aq.), toluene, 97 °C, 16 h. f) bromobenzene, 1 h, then phenylboronic acid, 1 h.

Compared to the HOMO level (−5.25 eV) of PCDTBT obtained under identical experimental conditions, that of PCX3 is 0.15 eV lower, which offers the possibility of V_{oc} enhancement in devices comprising fullerene acceptors.^[35]

Solar cell devices with a structure of ITO/PEDOT:PSS/PCX3:PC₇₁BM/Al were prepared and characterized under an inert atmosphere. We first investigated the device performance with different PCX3/PC₇₁BM weight ratios under AM

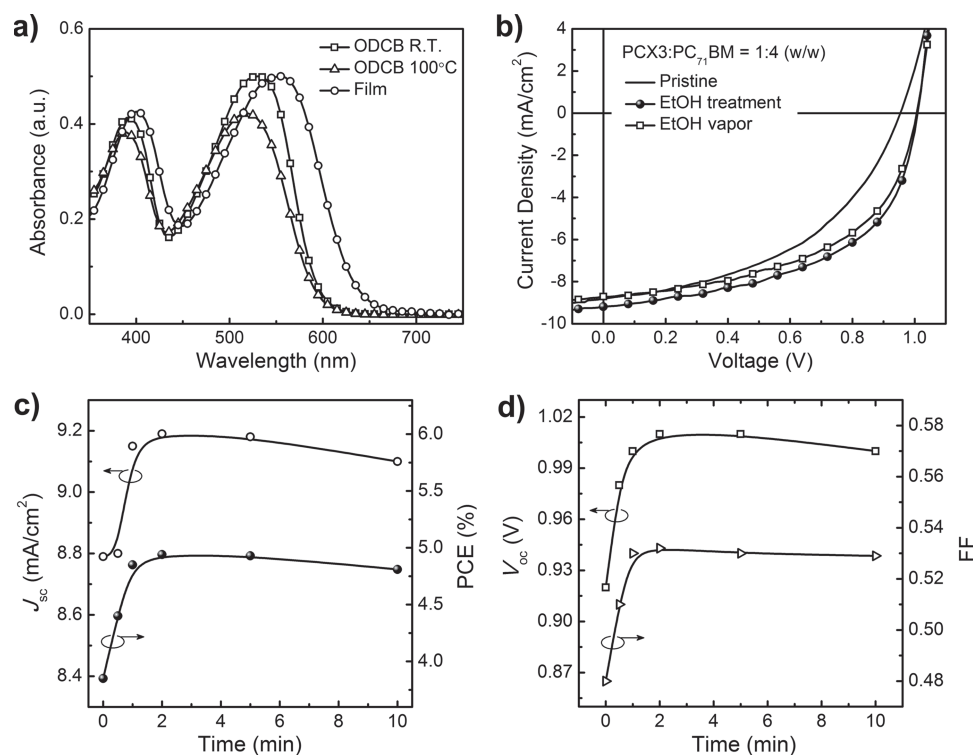


Figure 1. (a) UV-vis absorption spectra of PCX3 in ODCB and solid state. (b) J - V characteristics of 1:4 PCX3/PC₇₁BM devices before and after ethanol treatment. (c, d) Wetting time-dependent photovoltaic characteristics of the devices upon ethanol treatment.

Table 1. Summary of characteristics for PCX3/PC₇₁BM BHJ solar cells.

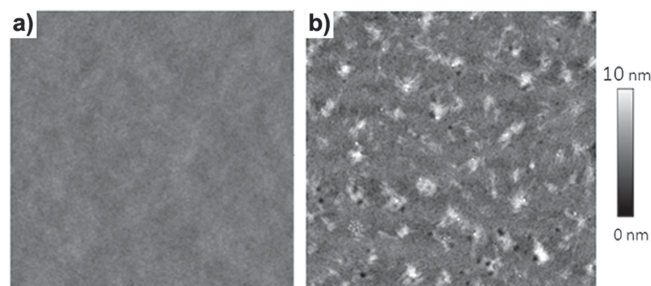
PCX3/PC ₇₁ BM (w/w ratio)	J_{sc} [mA/cm ²]	V_{oc} [V]	FF [%]	PCE [%] avg	PCE [%] best
1:1	5.6 ± 0.2	0.86 ± 0.02	34.8 ± 1	1.69	1.85
1:2	7.6 ± 0.2	0.92 ± 0.01	38.6 ± 1	2.71	2.90
1:3	8.5 ± 0.2	0.96 ± 0.01	45.2 ± 1	3.67	3.79
1:4	8.8 ± 0.2	0.96 ± 0.01	46.5 ± 1	3.90	3.96

1.5G at 100 mW/cm² conditions (Figure S5); **Table 1** provides a summary of the results. The optimized weight ratio of PCX3 to PC₇₁BM was found to be 1:4, yielding a device with V_{oc} = 0.96 V and PCE = 3.9%. The film thickness of this device was approximately 100 nm. Although the performance of solar cells with weight ratios of 1:1 and 1:2 are considerably lower, the behaviour of devices with ratios of 1:3 and 1:4 are comparable. The higher V_{oc} as compared with PCDTBT (0.88 V)^[22] agrees with a lower-lying HOMO level, as determined by electrochemistry. The EQE curve from the best device reveals broad photoresponse from 300 nm to 700 nm, with a maximum value of 74% around 400 nm. The J_{sc} calculated from EQE curve under standard AM 1.5G conditions yields 8.8 mA/cm², which is in accordance with that obtained from J - V measurements.

We found that the fill factor (FF) of the 1:4 PCX3/PC₇₁BM devices can be improved by treatment with ethanol as follows: (i) ethanol was added atop the active layer, (ii) solvent was removed by spin coating, (iii) the resulting film was placed under vacuum overnight, and (iv) the cathode was evaporated. With this ethanol treatment the FF increases from 46% to 53%, leading to a PCE of 5.1%. The J - V characteristics of solar cells with and without ethanol treatment are illustrated in Figure 1b. An increase of V_{oc} can also be observed, from 0.96 to 1.01 V, as well as J_{sc} from 8.8 to 9.2 mA/cm². The EQE spectra are in agreement with the increase of J_{sc} (Figure S6). It is also worth pointing out that other polar solvents, including acetonitrile and methanol, have positive effects on device efficiencies with only slightly lower PCEs compared to ethanol (Figure S7 and Table S1). There is therefore a range of solvent options available to execute this post treatment improvement.

The wetting time of ethanol (*i.e.* the time that ethanol is present on top of active layer before the substrate is spun) is relevant for the observed improvements. Figure 1c and 1d present the wetting time dependence of J_{sc} , V_{oc} , FF, and overall PCE of 1:4 PCX3/PC₇₁BM devices upon ethanol treatment, see also Table S2. A wetting time of 2 min was found to work best. Although there are slight decreases of PCE with wetting time longer than 2 min, the V_{oc} and FF remain around 1.0 V and 53%, respectively. In a parallel experiment, the devices were exposed to ethanol vapour by simply introducing the device into a beaker with ethanol (no direct contact between ethanol and the device surface). One observes that these devices also show comparable increase in FF to 53% (Figure 1b). These observations suggest that the spin-casted ethanol treatment does not wash away any surface-accumulated components, *i.e.* it does not simply serve the role of “cleaning” the surface.

J - V characteristics were also carried out under dark conditions (Figure S8). The current density of the ethanol-treated

**Figure 2.** AFM height images (2 μm × 2 μm) of PCX3/PC₇₁BM blend films before (a) and after (b) ethanol treatment.

device is suppressed in the region between -1.0 and 1.0 V. The shunt resistance (R_{sh}) was calculated as $5.3 \times 10^5 \Omega \cdot \text{cm}^2$ and $1.3 \times 10^6 \Omega \cdot \text{cm}^2$ for the pristine and ethanol treated devices, respectively. These data are in agreement with the decreased leakage current and slightly increased V_{oc} in the devices. Moreover, the series resistance (R_s) of the ethanol-treated device is $17 \Omega \cdot \text{cm}^2$, which is lower than for a pristine device ($62 \Omega \cdot \text{cm}^2$). These results indicate that better diode characteristics were obtained after simple ethanol treatment.

Surface topographic features as function of ethanol treatment were examined by atomic force microscopy (AFM). The pristine 1:4 PCX3/PC₇₁BM film exhibits a homogeneous, relatively flat surface (**Figure 2a**) with a root-mean-squared (RMS) surface roughness of 0.3 nm. Ethanol treatment causes slight roughening; RMS = 1.2 nm (**Figure 2b**). However, there is no observable change in the film thickness, as determined by profilometry. Similar roughness increases were observed in films treated with acetonitrile or methanol, with RMS values of 0.7 and 1.3 nm, respectively (**Figure S9**). It is also worth noting that no obvious changes were observed in the absorption spectra of 1:4 PCX3/PC₇₁BM films after ethanol treatment (**Figure S10**), unlike the case of P3HT/PCBM blends.^[30] This observation suggests the absence of obvious reconstruction of the internal donor structure. In agreement, we find nearly identical features in the X-ray diffraction (XRD) measurements (**Figure S11**).

Further additional experiments were carried out to probe the origin of the ethanol effect. In particular, PEDOT:PSS is known to be sensitive to polar solvents.^[36,37] A simple control experiment was done by spin-coating 1:4 PCX3/PC₇₁BM atop PEDOT:PSS that had been previously treated with ethanol. Sharp decreases in V_{oc} and FF were observed (**Figure S12**). A parallel experiment was performed by using thermally evaporated MoO_x as the ITO/PCX3/PC₇₁BM interlayer. As shown in **Figure 3**, ethanol treatment does not provide the improvements observed with the PEDOT:PSS-containing device. This collected set of observations indicates that part of the improvement arises from modification of the PEDOT:PSS/BHJ interface, but whatever modifications are occurring need this interface to be created ahead of time.

As a final set of experiments, we used ultraviolet photoelectron spectroscopy (UPS) to probe how ethanol treatment modifies an organic/metal interface. Because of experimental limitations, a testing structure different from the device configuration had to be used. Specifically, PCX3/PC₇₁BM blend solution was spin-coated atop gold substrates. We recognize that the

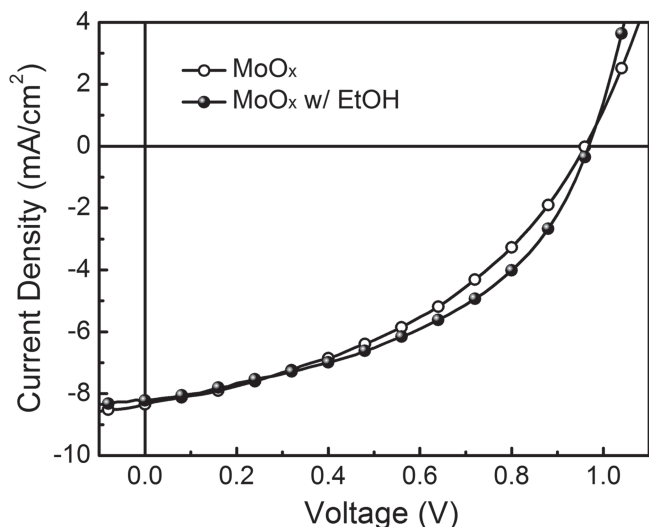


Figure 3. *J*-*V* characteristics of PCX3/PC₇₁BM (1:4) devices before and after solvent treatment by using MoO_x as an anode buffer layer.

BHJ/Au interface is not identical to those in the solar cell device. Nonetheless it provides a useful platform to examine ethanol diffusion through the film. **Figure 4a** shows the UPS spectra taken for the pristine and ethanol treated films. The abscissa

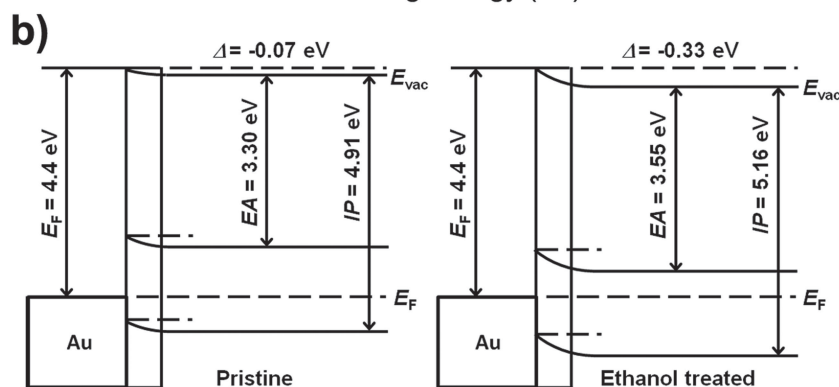
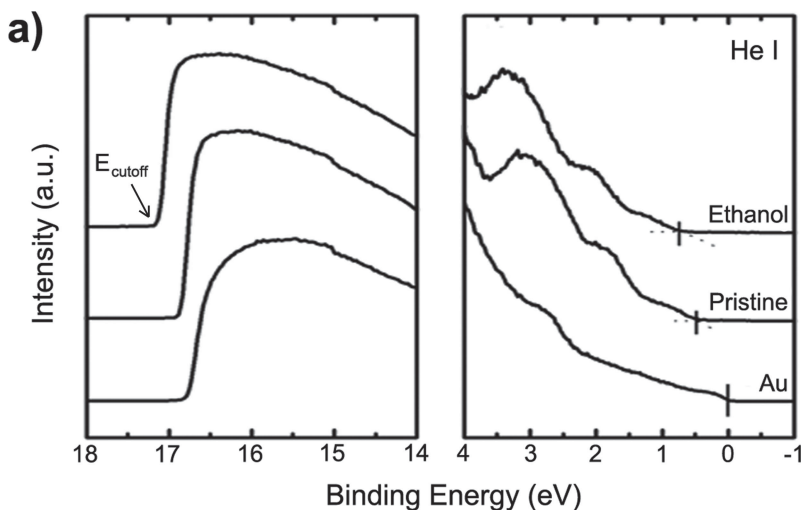


Figure 4. (a) UPS spectra of Au, pristine film and ethanol treated film. (b) Energy diagrams near the organic/metal interface. EA is electron affinity. IP is ionization potential.

is the binding energy relative to the work function (E_F) of Au, which is defined by the energy of the electron before excitation relative to the vacuum level (E_{vac}).^[38] The E_{vac} of the films were determined by linear extrapolation of the secondary electron cut-offs on the high-binding-energy side of the spectra (14–18 eV). The shift in E_{vac} indicates the magnitude of the interfacial dipole (Δ).^[39] For the pristine film, an interfacial dipole of 0.07 eV was obtained. Upon ethanol treatment, the value increases to 0.33 eV. The energy diagrams of the organic/metal interface are illustrated in Figure 4b. We take these features to indicate that ethanol can penetrate the PCX3/PC₇₁BM (even in the absence of obvious solubility) to considerably influence the contact properties of a “buried” interface.

In conclusion, a novel arylated-carbazole comonomer has been developed and successfully incorporated in the conjugated polymer PCX3. This aryl substituent offers the potential to tailor the optical and electronic properties of the polymers, and is particularly suited for modifying the HOMO energy level. The high molecular weight polymer exhibits excellent solubility and film-formation property. In combination with PC₇₁BM one can obtain solar cells with V_{oc} of 0.96 V and a PCE of 3.9%. It was also determined that post treatment of the preformed BHJ thin film with ethanol, which is nontoxic, offers a simple method for improving the overall device efficiency and may offer opportunities to be incorporated in high throughput fabrication. How

this process works remains poorly understood. There are obvious minor changes to the surface topography, which suggest possible modification of the top metal contact. However, we find the unexpected observation that (a) swelling by ethanol is sufficient for attaining the improvements, and (b) evidence that the swelling changes the properties of the buried PEDOT:PSS/BHJ interface. Further understanding and optimization of this interfacial tuning has the potential to improve materials performance in a wide range of BHJ structures.

Experimental Section

Characterization: ¹H and ¹³C NMR were carried out using a Bruker Avance 500 spectrometer in appropriate deuterated solvents at room temperature (298 K) unless otherwise noted. Chemical shifts were recorded as δ value (ppm) relative to trace solvent signals.^[40] Mass spectra were taken from a Shimadzu GC-17A MS-QP5000 and a VG70 Magnetic Sector instrument. UV-visible absorption spectra were collected on a Perkin Elmer Lambda 750 spectrophotometer at different temperature. Number-average molecular weight (M_n) and weight-average molecular weight (M_w) were determined by a Polymer Laboratories PL220 instrument at high temperature. Cyclic voltammograms (CVs) were performed on a CHI 730B instrument in a standard three-electrode, one compartment configuration equipped with Ag/AgCl reference electrode, platinum counter electrode and glassy carbon working electrode (dia. 3 mm). Glassy carbon electrodes were polished with alumina before

use. The CV curves were recorded in anhydrous acetonitrile (CH_3CN) with 0.1 M tetrabutylammonium hexafluorophosphate ($n\text{-Bu}_4\text{NPF}_6$) as the supporting electrolyte at scan rate $100\text{ mV}\cdot\text{s}^{-1}$. All solutions were purged with dry argon for 15 minutes to deoxygenate the system. Films were prepared by drop-casting a mixture of PCX3 in dry chloroform ($\sim 2\text{ mg}\cdot\text{mL}^{-1}$) onto glassy carbon electrode under room temperature. Fc/Fc^+ was taken as an internal standard.

Synthetic procedures: All reagents and chemicals were purchased from Alfa and Sigma-Aldrich and used without further purification. All solvents used for reaction here were redistilled following standard procedures. Column chromatography was carried out on flash silica gel (32–63 μ , Dynamic Adsorbents Inc.). The 1-iodo-3,5-dimethoxybenzene (**1**),^[41] 2,7-dibromocarbazole (**2**)^[42] and 4,7-bis(5-bromothiophen-2-yl)-5,6-bis(octyloxy)-2,1,3-benzothiadiazole (**7**)^[32] have already been prepared in the literature. All other compounds were synthesized following procedures described below.

***N*-9'-(3,5-Dimethoxyphenyl)-2,7-dibromocarbazole (3):** To a 100 mL round bottom flask was charged 2,7-dibromocarbazole (4.0 g, 12.3 mmol, 1.0 eq), 1-iodo-3,5-dimethoxybenzene (3.9 g, 14.8 mmol, 1.2 eq), potassium phosphate (7.82 g, 36.9 mmol, 3.0 eq), copper iodide (0.586 g, 3.1 mmol, 0.25 eq). The solid mixture was purged with argon before adding anhydrous dioxane (30 mL). The mixture was stirred at room temperature for 15 min, then (\pm)-trans-1,2-diaminocyclohexane (0.72 mL, 0.5 eq) was added rapidly and the reaction was heated at reflux overnight. The mixture was then filtered and washed with dichloromethane. After removing the solvent, the crude product was first purified by column chromatography (silica gel, 15% DCM in hexane as eluent), then dissolved as-obtained solid in a small amount of boiling chloroform. The title compound (4.2 g, yield: 73%) was obtained as an off-white solid by precipitation chloroform solution in methanol (200 mL). It should be noted that less than 4% of the compound was mono-iodized and could not be separated.

¹H NMR (500 MHz, CDCl_3 , δ): 7.95–7.93 (d, $J = 10.0\text{ Hz}$, 2H), 7.56 (s, 2H), 7.41–7.39 (d, $J = 10.0\text{ Hz}$, 2H), 6.64–6.62 (m, 3H), 3.87 (s, 6H). ¹³C NMR (125 MHz, CDCl_3 , δ): 162.1, 141.9, 138.2, 129.4, 123.8, 121.7, 120.3, 113.4, 105.6, 100.8, 55.8. EI-MS: Calculated for $\text{C}_{20}\text{H}_{15}\text{Br}_2\text{NO}_2$: 460.94, Found: 461.00.

***N*-9'-(3,5-Dihydroxyphenyl)-2,7-dibromocarbazole (4):** To a 100 mL flask was added compound **3** (4.0 g, 8.68 mmol, 1.0 eq) and DCM (50 mL). The clear solution was purged with argon for 30 min before cooled to $-78\text{ }^\circ\text{C}$ using an acetone/dry ice bath. BBr_3 (6.52 g, 26.0 mmol, 3.0 eq) was dissolved in methylene chloride (20 mL) under argon atmosphere and was added dropwise to the mixture in 10 min. The reaction was allowed to warm to room temperature and stirred for 2 days. The reaction mixture was then quenched with water carefully, extracted with methylene chloride three times. The organic layer was washed with water and dried over magnesium sulfate. The solvent was removed under reduced pressure. The residue was purified by column chromatography (silica gel, 5% ethyl acetate in methylene chloride as eluent). Compound **4** (2.56 g, 68%) was obtained as a white solid.

¹H NMR (500 MHz, CDCl_3 , δ): 7.89–7.87 (d, $J = 10.0\text{ Hz}$, 2H), 7.57 (s, 2H), 7.35–7.33 (d, $J = 10.0\text{ Hz}$, 2H), 6.56–6.53 (m, 3H). ¹³C NMR (125 MHz, CDCl_3 , δ): 159.2, 141.6, 137.7, 123.2, 121.8, 121.4, 113.0, 105.6, 103.1. EI-MS: Calculated for $\text{C}_{18}\text{H}_{11}\text{Br}_2\text{NO}_2$: 430.92, Found: 430.35.

***N*-9'-(3,5-Bis(octyloxy)phenyl)-2,7-dibromocarbazole (5):** A suspension of compound **4** (1.5 g, 3.5 mmol, 1.0 eq), 1-bromooctane (3.6 mL, 21.0 mmol, 6.0 eq), and potassium carbonate (5.8 g, 42 mmol, 12.0 eq) in dry *N,N*-dimethylformamide (15 mL) was degassed for three times. The mixture was stirred at $70\text{ }^\circ\text{C}$ for 5 h monitored by thin layer chromatography (TLC). The suspension was then cooled to room temperature and filtered off. The filtrate was directly loaded on silica gel column, first using pure hexane as eluent to remove *N,N*-dimethylformamide, then using 10% methylene chloride in hexane as eluent. The title compound (2.1 g, 92%) was collected as a white powder after removal of solvents.

¹H NMR (500 MHz, CDCl_3 , δ): 7.93–7.91 (d, $J = 10.0\text{ Hz}$, 2H), 7.54 (s, 2H), 7.39–7.37 (d, $J = 10.0\text{ Hz}$, 2H), 6.59–6.57 (m, 3H), 3.99–3.97 (t, $J = 5.0\text{ Hz}$, 4H), 1.82–1.79 (m, 4H), 1.48–1.44 (m, 4H), 1.38–1.26 (m, 16H),

0.90–0.87 (t, $J = 7.0\text{ Hz}$, 6H). ¹³C NMR (125 MHz, CDCl_3 , δ): 161.6, 142.0, 138.0, 123.7, 121.7, 121.6, 120.1, 113.5, 105.9, 101.5, 68.6, 31.9, 29.5, 29.4, 29.3, 26.2, 22.8, 14.2. FI-TOF-MS: Calculated for $\text{C}_{34}\text{H}_{43}\text{Br}_2\text{NO}_2$: 657.17, Found: 657.16.

2,7-Bis(4',4',5',5'-tetramethyl-1',3',2'-dioxaborolan-2'-yl)-*N*-9'-(3,5-bis(octyloxy)phenyl)carbazole (6): To a stirred solution of **5** (1.2 g, 1.8 mmol, 1.0 eq) in dry THF (60 mL) at $-78\text{ }^\circ\text{C}$ under an inert atmosphere was added dropwise a solution of *n*-BuLi (2.9 mL, 1.6 M in hexane, 4.6 mmol, 2.5 eq). The resulting mixture was stirred at $-78\text{ }^\circ\text{C}$ for 2 h to form a thick suspension, after which 2-isopropoxy-4,4,5,5-tetramethyl-1,3,2-dioxaborolane (1.1 mL, 5.5 mmol, 3.0 eq) was added all at once. The reaction mixture was stirred for an additional hour before slowly brought to room temperature and stirred overnight. The mixture was then poured into water, extracted with diethyl ether three times. The organic layer was washed with brine, water and dried over magnesium sulfate. After the solvent was removed, the residue was purified on a silica gel column using 3% ethyl acetate in hexane as eluent. Monomer **6** (0.95 g, 69%) was obtained as a white solid after recrystallization in ethanol.

¹H NMR (500 MHz, CDCl_3 , δ): 8.17–8.15 (d, $J = 7.5\text{ Hz}$, 2H), 7.87 (s, 2H), 7.75–7.73 (d, $J = 8.0\text{ Hz}$, 2H), 6.68–6.67 (m, 2H), 6.61–6.60 (m, 1H), 4.00–3.98 (t, $J = 6.5\text{ Hz}$, 4H), 1.83–1.80 (m, 4H), 1.49–1.45 (m, 4H), 1.36–1.25 (m, 40H), 0.90–0.87 (t, $J = 6.5\text{ Hz}$, 6H). ¹³C NMR (125 MHz, CDCl_3 , δ): 161.3, 141.3, 139.2, 126.0, 125.6, 120.0, 116.7, 106.6, 83.9, 68.6, 31.9, 29.5, 29.4, 26.2, 25.0, 22.8, 14.2. FI-TOF MS: Calculated for $\text{C}_{46}\text{H}_{67}\text{B}_2\text{NO}_6$: 751.52, Found: 751.49.

Poly[*N*-9'-(3,5-Bis(octyloxy)phenyl)-2,7-carbazole-*alt*-5,5-(4',7'-dithienyl-5',6'-bis(octyloxy)-2',1',3'-benzothiadiazole)] (PCX3): To a 20 mL flame dried reaction vial was added monomer **6** (375.8 mg, 0.5 mmol, 1.0 eq) and 4,7-bis(5-bromothiophen-2-yl)-5,6-bis(octyloxy)-2,1,3-benzothiadiazole (**7**) (357.3 mg, 0.5 mmol, 1.0 eq), tris(dibenzylideneacetone)dipalladium(0) (15 mg, 0.016 mmol, 0.033 eq) and tri(*o*-tolyl)phosphine (25 mg, 0.082 mmol, 0.164 eq) equipped with a magnetic stirring bar under a nitrogen atmosphere. Dry toluene (5 mL) was added and the reaction vial was sealed. A pre-degassed aqueous tetraethylammonium hydroxide (20%, 2.0 mL) was added. The reaction mixture was then stirred at $97\text{ }^\circ\text{C}$ for 16 h on a conventional oil bath. Bromobenzene (60 μL) was added to the mixture and after 1 h, a solution of phenylboronic acid (60 mg) in toluene (0.7 mL) was added. Polymer end-capping was done in 2 h. The polymer was purified by precipitation in methanol (300 mL), filtered, and subjected to Soxhlet extraction with methanol (12 h), acetone (5 h), hexane (12 h) and chloroform (3 h). After the chloroform fraction was concentrated to c.a. 100 mL, *N,N*-diethylphenylazothioformamide (35.4 mg, 0.16 mmol, 0.32 eq) was added as a palladium scavenger. The mixture was stirred at $60\text{ }^\circ\text{C}$ for 2 h under argon, followed by precipitation in methanol (300 mL), filtered, and wash with methanol. The polymer was then dissolved in chloroform (50 mL) and precipitated in methanol a second time. The pure polymer (484 mg, 92%) was collected as a black purple solid after filtration and dried in a vacuum oven.

¹H NMR (500 MHz, CDCl_3 , δ): 8.50 (br, 2H), 8.14–8.13 (d, $J = 5.0\text{ Hz}$, 2H), 7.78 (br, 2H), 7.69–7.68 (d, $J = 5.0\text{ Hz}$, 2H), 7.48 (br, 2H), 6.79 (br, 2H), 6.66 (br, 2H), 4.19 (br, 4H), 4.04 (br, 4H), 1.99–1.97 (m, 4H), 1.88–1.83 (m, 4H), 1.54–1.46 (m, 8H), 1.35–1.26 (m, 32H), 0.91–0.88 (m, 12H). $M_n = 65\text{ kDa}$, PDI = 2.5.

Photovoltaic device Fabrication and Characterization: Polymer solar cell devices with a sandwiched structure of glass/ITO/PEDOT:PSS/PCX3:PCBM/Aluminium were prepared according to the following procedure. ITO-coated glass substrates were first ultrasonicated with detergent, deionized water, acetone, and isopropyl alcohol for 30 min, respectively. The substrates were subsequently treated with UV/ozone for 20 min. PEDOT:PSS (Bayer Baytron 4083) layer was then spin-coated on top of the ITO substrate with a thickness of $\sim 40\text{ nm}$ by using a $0.45\text{ }\mu\text{m}$ filter, and subsequently dried at $140\text{ }^\circ\text{C}$ for 10 min in air. The active layer, with a thickness around 100 nm was then spin-coated atop PEDOT:PSS layer by using a CB:ODCB (1:3 v/v) solution with different blend ratios of PCX3 and PC₇₁BM (1:1, 1:2, 1:3 and 1:4 w/w, 10 mg·mL⁻¹ of PCX3) under an inert atmosphere. The film thickness was controlled by adjusting the spin speed between 800 and 2500 rpm. The films

were dried at 70 °C for 10 min before directly subjected to thermal evaporation or post solvent treatment. Polar solvent was spin-coated at 2000 rpm on top of the active layer for 60 s. The solvents used here were purchased from Sigma-Aldrich without further purification. For the parallel experiments, thermally evaporated MoO_x anode buffer layer on ITO with thickness around 10 nm was used instead of PEDOT:PSS. The thickness of PEDOT:PSS layer and active layer was determined by a surface profilometer (Alfa step-500, Tencor). Finally, a 100 nm thick Al layer was thermally evaporated through a shadow mask under a pressure of 10⁻⁶ Torr. There were two devices on one single substrate and each with an active area of 0.13 cm². Photovoltaic characterization was performed on a Keithley 2602 source measure unit with a 300 W Xe arc lamp and an AM 1.5 global filter. The solar simulator illumination intensity was measured using a KG1 filter from the National Renewable Energy Laboratory (NREL) with silicon photovoltaics. External quantum efficiency (EQE) spectra were measured using a 75 W Xe lamp, Newport monochromator, Newport optical chopper, and a Stanford Research Systems lock-in amplifier. Power-density calibration was done by National Institute of Standards and Technology traceable silicon photodiode.

UPS Measurement: A gold film of 75 nm was deposited on a pre-cleaned Si substrate with a thin native oxide. Solutions containing PCX3:PC₇₁BM (1:4) in CB:DCB (1:3) mixed solvent with a concentration of 2 mg mL⁻¹ were then spin-cast on top of the Au film. For the film that underwent ethanol treatment, ethanol was present on top of the active layer for 2 min. Film fabrication was carried out in a N₂-atmosphere glovebox. To minimize the possibility of exposure to air the films were then transferred from the N₂-atmosphere dry box to the analysis chamber inside an air-free sample holder. Subsequently, the samples were kept inside a high-vacuum chamber overnight to remove solvent. The UPS analysis chamber was equipped with a hemispherical electron-energy analyzer (Kratos Ultra spectrometer), and was maintained at 1.33 × 10⁻⁷ Pa. The UPS was measured using He I (*hν* = 21.2 eV) source, and the electron energy analyzer was operated at a constant pass energy of 10 eV. During the measurements, a sample bias of -9 V was used in order to separate the sample and the secondary edge for the analyzer. In order to confirm the reproducibility of UPS spectra, we repeated these measurements twice on two sets of samples.

Supporting Information

Supporting Information is available from the Wiley Online Library or from the author.

Acknowledgements

The authors are grateful to the Department of Energy BES and the Air Force Office of Scientific Research for support of this work.

Received: April 19, 2012

Published online:

- [1] G. Yu, J. Gao, J. C. Hunnellen, F. Wudl, A. J. Heeger, *Science* **1995**, *270*, 1789.
- [2] B. C. Thompson, J. M. J. Fréchet, *Angew. Chem., Int. Ed.* **2008**, *47*, 58.
- [3] M. A. Green, K. Emery, Y. Hishikawa, W. Warta, *Prog. Photovolt. Res. Appl.* **2010**, *18*, 144.
- [4] Y.-J. Cheng, S.-H. Yang, C.-S. Hsu, *Chem. Rev.* **2009**, *109*, 5868.
- [5] B. Carsten, F. He, H. J. Son, T. Xu, L. Yu, *Chem. Rev.* **2011**, *111*, 1493.
- [6] J. Chen, Y. Cao, *Acc. Chem. Res.* **2009**, *42*, 1709.
- [7] G. Li, C. W. Chu, V. Shrotriya, J. Huang, Y. Yang, *Appl. Phys. Lett.* **2006**, *88*, 253503.
- [8] J. Y. Kim, K. Lee, N. E. Coates, D. Moses, T.-Q. Nguyen, M. Dante, A. J. Heeger, *Science* **2007**, *317*, 222.
- [9] L. Yang, H. Zhou, S. C. Price, W. You, *J. Am. Chem. Soc.* **2012**, *134*, 5432.
- [10] F. G. Brunetti, X. Gong, M. Tong, A. J. Heeger, F. Wudl, *Angew. Chem., Int. Ed.* **2010**, *49*, 532.
- [11] C. L. Chochos, S. P. Economopoulos, V. Deimede, V. G. Gregoriou, M. T. Lloyd, G. G. Malliaras, J. K. Kallitsis, *J. Phys. Chem. C* **2007**, *111*, 10732.
- [12] P. Sonar, G.-M. Ng, T. T. Lin, A. Dodabalapur, Z.-K. Chen, *J. Mater. Chem.* **2010**, *20*, 3626.
- [13] N. Blouin, A. Michaud, M. Leclerc, *Adv. Mater.* **2007**, *19*, 2295.
- [14] Q. Zheng, B. J. Jung, J. Sun, H. E. Katz, *J. Am. Chem. Soc.* **2010**, *132*, 5394.
- [15] L. Huo, J. Hou, S. Zhang, H.-Y. Chen, Y. Yang, *Angew. Chem., Int. Ed.* **2010**, *49*, 1500.
- [16] K.-H. Ong, S.-L. Lim, H.-S. Tan, H.-K. Wong, J. Li, Z. Ma, L. C. H. Moh, S.-H. Lim, J. C. de Mello, Z.-K. Chen, *Adv. Mater.* **2011**, *23*, 1409.
- [17] E. Wang, M. Wang, L. Wang, C. Duan, J. Zhang, W. Cai, C. He, H. Wu, Y. Cao, *Macromolecules* **2009**, *42*, 4410.
- [18] T.-Y. Chu, J. Lu, S. Beaupré, Y. Zhang, J.-R. Pouliot, S. Wakim, J. Zhou, M. Leclerc, Z. Li, J. Ding, Y. Tao, *J. Am. Chem. Soc.* **2011**, *133*, 4250.
- [19] S. C. Price, A. C. Stuart, L. Yang, H. Zhou, W. You, *J. Am. Chem. Soc.* **2011**, *133*, 4625.
- [20] J. Li, F. Dierschke, J. Wu, A. C. Grimsdale, K. Müllen, *J. Mater. Chem.* **2006**, *16*, 96.
- [21] N. Blouin, A. Michaud, D. Gendron, S. Wakim, E. Blair, R. Neagu-Plesu, M. Belletête, G. Durocher, Y. Tao, M. Leclerc, *J. Am. Chem. Soc.* **2007**, *130*, 732.
- [22] S. H. Park, A. Roy, S. Beaupre, S. Cho, N. Coates, J. S. Moon, D. Moses, M. Leclerc, K. Lee, A. J. Heeger, *Nat. Photon.* **2009**, *3*, 297.
- [23] J. Li, A. C. Grimsdale, *Chem. Soc. Rev.* **2010**, *39*, 2399.
- [24] A. J. Moulé, K. Meerholz, *Adv. Funct. Mater.* **2009**, *19*, 3028.
- [25] T. M. Clarke, J. R. Durrant, *Chem. Rev.* **2010**, *110*, 6736.
- [26] J. Peet, J. Y. Kim, N. E. Coates, W. L. Ma, D. Moses, A. J. Heeger, G. C. Bazan, *Nat. Mater.* **2007**, *6*, 497.
- [27] G. Li, V. Shrotriya, J. Huang, Y. Yao, T. Moriarty, K. Emery, Y. Yang, *Nat. Mater.* **2005**, *4*, 864.
- [28] S. Miller, G. Fanchini, Y.-Y. Lin, C. Li, C.-W. Chen, W.-F. Su, M. Chhowalla, *J. Mater. Chem.* **2008**, *18*, 306.
- [29] J. H. Seo, A. Gutacker, Y. Sun, H. Wu, F. Huang, Y. Cao, U. Scherf, A. J. Heeger, G. C. Bazan, *J. Am. Chem. Soc.* **2011**, *133*, 8416.
- [30] H. Li, H. Tang, L. Li, W. Xu, X. Zhao, X. Yang, *J. Mater. Chem.* **2011**, *21*, 6563.
- [31] S. Nam, J. Jang, H. Cha, J. Hwang, T. K. An, S. Park, C. E. Park, *J. Mater. Chem.* **2012**, *22*, 5543.
- [32] R. Qin, W. Li, C. Li, C. Du, C. Veit, H.-F. Schleiermacher, M. Andersson, Z. Bo, Z. Liu, O. Inganäs, U. Wuerfel, F. Zhang, *J. Am. Chem. Soc.* **2009**, *131*, 14612.
- [33] J. K. Park, J. Jo, J. H. Seo, J. S. Moon, Y. D. Park, K. Lee, A. J. Heeger, G. C. Bazan, *Adv. Mater.* **2011**, *23*, 2430.
- [34] K. T. Nielsen, K. Bechgaard, F. C. Krebs, *Macromolecules* **2005**, *38*, 658.
- [35] M. C. Scharber, D. Mühlbacher, M. Koppe, P. Denk, C. Waldauf, A. J. Heeger, C. J. Brabec, *Adv. Mater.* **2006**, *18*, 789.
- [36] Y. Xia, J. Ouyang, *J. Mater. Chem.* **2011**, *21*, 4927.
- [37] B. Peng, X. Guo, C. Cui, Y. Zou, C. Pan, Y. Li, *Appl. Phys. Lett.* **2011**, *98*, 243308.
- [38] J. H. Seo, T.-Q. Nguyen, *J. Am. Chem. Soc.* **2008**, *130*, 10042.
- [39] J. H. Seo, R. Yang, J. Z. Brzezinski, B. Walker, G. C. Bazan, T.-Q. Nguyen, *Adv. Mater.* **2009**, *21*, 1006.
- [40] G. R. Fulmer, A. J. M. Miller, N. H. Sherden, H. E. Gottlieb, A. Nudelman, B. M. Stoltz, J. E. Bercaw, K. I. Goldberg, *Organometallics* **2010**, *29*, 2176.
- [41] J. Zhao, R. C. Larock, *J. Org. Chem.* **2006**, *71*, 5340.
- [42] A. W. Freeman, M. Urvoy, M. E. Criswell, *J. Org. Chem.* **2005**, *70*, 5014.